FT-IR Difference Spectroscopy Elucidates Crucial Interactions of Sensory Rhodopsin I with the Cognate Transducer HtrI

Olga S. Mironova,[‡,||] Ivan L. Budyak,[‡,||] Georg Büldt,[‡] Ramona Schlesinger,[*,‡] and Joachim Heberle[§]

Research Center Jülich, Institute for Structural Biology (IBI-2), 52425 Jülich, Germany, and Department of Chemistry, Biophysical Chemistry (PC III), Bielefeld University, 33615 Bielefeld, Germany

Received March 23, 2007; Revised Manuscript Received June 14, 2007

ABSTRACT: The phototaxis receptor sensory rhodopsin I (SRI) from *Halobacterium salinarum* interacts with its cognate transducer (HtrI) forming a transmembrane complex. After light excitation of the chromophore all-*trans* retinal, SRI undergoes structural changes that are ultimately transmitted to HtrI. The interaction of SRI with HtrI results in the closure of the receptor's proton pathway, which renders the photocycle recovery kinetics of SRI pH-independent. We demonstrate on heterologously expressed and reconstituted SRI-HtrI fusion proteins that the transmembrane part of HtrI (residues 1−52) as well as the downstream cytoplasmic part (residues 53−147) exhibit conformational changes after light excitation. The sum of these conformational changes is similar to those observed in the fusion constructs SRI-HtrI 1−71 and SRI-HtrI 1−147, which display pH-independent receptor kinetics. These results indicate the occurrence of spatially distinct conformational changes that are required for functional signal transmission. Kinetic and spectroscopic analysis of HtrI point mutants of Asn53 provides evidence that this residue is involved in the receptor−transducer interaction. We suggest that Asn53 plays a role similar to that of Asn74 of the HtrII from *Natronobacterium pharaonis*, the latter forming a hydrogen bond to the receptor within the membrane.

Sensory rhodopsin I (SRI[1]) (*1*) from the archaeon *Halobacterium salinarum* is a member of the family of seven-transmembrane (TM) retinal-containing proteins. Bacteriorhodopsin and halorhodopsin both are light-driven ion pumps, the former acts as an outward proton pump, and the latter is an inward chloride pump. SRI and SRII are photoreceptor proteins responsible for positive and/or negative phototaxis (*2*). SRI mediates attractant as well as repellent phototaxis responses to orange and near-UV light, respectively. The chromophore, all-*trans* retinal, is bound to a Lys side chain and forms a protonated Schiff base. Photon absorption by the receptor's ground state, SR_{587}, leads to retinal isomerization around the C_{13}═C_{14} bond, Schiff base deprotonation, and formation of the signaling state, SR_{373} (also referred to as M state). If no blue photon is absorbed, SR_{373} decays back directly to the ground state, thus providing the attractant response, while blue photon absorption by SR_{373} results in the repellent response (*3*). The 536 amino acid long halobacterial transducer I (HtrI) comprises two TM α-helices followed by an extended cytoplasmic part (*4*). Tight coupling of the receptor to its transducer protein in a 2:2 complex (*5*) is necessary for downstream signal transduction (*6*). HtrI modulates the photochemical properties of SRI. The lifetime of SR_{373} in the absence of HtrI has been demonstrated to be strongly pH-dependent, whereas it is almost constant in complex with the transducer (*6*, *7*). The pH dependence of the M state decay kinetics has been discussed in terms of the existence of the receptor's proton channel, which is closed in the presence of the bound transducer (*8*, *9*).

In contrast to the well-characterized negative phototaxis system from *Natronobacterium pharaonis* (*10*, *11*) consisting of SRII and its cognate transducer II, HtrII, high-resolution structural information is not available for the SRI-HtrI system. A number of recent studies investigated the roles of the various domains of the transducer in the formation of the SRI−HtrI complex and the subsequent signal transduction. The deletion of the residues 66−165 in the transducer cytoplasmic region has been demonstrated to recover the pH dependence of the M state decay of SRI (*12*). Perazzona et al. (*13*) reported that a deletion mutant of HtrI containing the residues 1−147 was sufficient to modulate the photocycle of SRI, while another mutant transducer molecule further shortened in this region until residue 124, left it unchanged. Later, on the basis of data obtained for chimeras of HtrI from *H. salinarum* and HtrII from *N. pharaonis*, Zhang et al. (*14*) found that the specificity of the SRI−HtrI interaction is mainly determined by the TM helices of the transducer. Recently, Chen and Spudich (*8*) have investigated the properties of fusion proteins consisting of SRI connected to truncated transducers via a flexible linker. The authors concluded that HtrI residues 62−66 were responsible for the closure of the SRI proton channel. Similarly, HtrII from *N. pharaonis* has been shown to interact directly with SRII in the membrane-proximal region (*15*).

* To whom correspondence should be addressed. Phone: +49 2461 612036. Fax: +49 2461 612020. E-mail: r.schlesinger@fz-juelich.de.

‡ Institute for Structural Biology (IBI-2).

§ Bielefeld University.

|| These authors equally contributed to this work.

[1] Abbreviations: SR, sensory rhodopsin; Htr, halobacterial transducer; SR_{587} and SR_{373}, SRI species with absorption maxima at 587 and 373 nm, respectively; TM, transmembrane; FT-IR, Fourier-transform IR; ATR, attenuated total reflectance; LED, light-emitting diode; MES, 2-(*N*-morpholino)ethanesulfonic acid; EDTA, ethylenediaminetetraacetic acid; DM, *n*-dodecyl-β-D-maltopyranoside.

10.1021/bi700563f CCC: $37.00
Published on Web 07/27/2007

Here, we studied chimeras of SRI fused to HtrI fragments of varying length. The fusion proteins were expressed in *E. coli*, purified, and reconstituted in lipids from halobacterial purple membranes. The SRI ground-state recovery kinetics was probed by UV/vis spectroscopy. The structural changes occurring after light excitation and the subsequent interactions between light receptor and transducer were investigated by FT-IR difference spectroscopy. This methodology has already been applied to the related SRII-HtrII system from *N. pharaonis* (*16*−*19*). We demonstrate that the transmembrane and the membrane-proximal cytoplasmic part of HtrI contribute independently to the interaction with SRI. We also examined the behavior of the SRI−HtrI complex with mutated Asn53 of HtrI, a hydrogen-bonding residue potentially involved in the receptor−transducer interaction. The exchange of Asn53 influences the communication between SRI and HtrI as gauged by the pH dependence of the receptor's ground-state recovery.

MATERIALS AND METHODS

Plasmids and Strains. For DNA manipulations, *E. coli* strain Top10 (Invitrogen) was used, and for gene expression, Epicurian Coli BL21-CodonPlus (DE3)-RP (Stratagene) was used. Both *sopI* and *htrI* genes were amplified by PCR from *H. salinarum* cells. Downstream of *sopI*, the coding region of the last 15 amino acids was removed (*20*) and replaced by coding sequences for 10 histidines to facilitate purification and a *Bcl*I site after the stop codon. Upstream of the gene, an *Nde*I site was introduced and the fragment coding for MDAV....HSES*HHHHHHHHHH* was cloned between the *Nde*I and *Bam*HI sites of the pET11a expression vector (Novagen). Thus, the construct used in this study and referred to further in the text as SRI is the His-tagged protein without the last 15 residues of the wild-type protein.

Chimeras consisting of SRI and parts of various lengths of HtrI (Figure 1) with a C-terminal His-tag were constructed with the megaprimer PCR method (*21*) and cloned into expression vectors of the pET series. The shortest construct, SRI-HtrI 1−52, represents the fusion with the predicted TM helices of HtrI (*22*). SRI-HtrI 1−71 contains additional cytoplasmic residues suggested to be involved in closing the proton channel of SRI (*8*). The longest fusion, SRI-HtrI 1−147, is designed in a manner analogous to that in the previous studies for SRI and HtrI deletion mutants separately expressed in *H. salinarum* (*13*). The SRI-HtrI 53−147 fusion is without the TM domain of the transducer.

To replace Asn53 by Asp, Ala, or Gln in SRI-HtrI 1−147, the triplet encoding Asn (AAC) was substituted by oligonucleotide-directed mutagenesis to GAT, GCA, or CAG, respectively.

Expression and Purification. For the production of SRI and its chimeras, *E. coli* BL21 (DE3) RP cells were transformed with the pET constructs and grown at 37 °C in double yeast tryptone medium supplemented by either 50 mg/L kanamycin or 200 mg/L ampicillin depending on the resistance gene of the expression vector. As soon as an OD_{600} of 0.6−0.8 was reached, 1 mM isopropyl-β-D-thiogalactopyranoside and 12 μM of all-*trans* retinal (Sigma) were added to induce expression and to supply the newly synthesized opsins with all-*trans* retinal, respectively. After 4 h of induction, the cells were harvested by centrifugation (10,000*g*). High expression levels were indicated by the intense blue color of the harvested cells, with an average yield of about 2 mg/L of cell culture. Purification was done essentially as described (*23*). Pelleted cells were resuspended in 500 mM NaCl, 50 mM MES at pH 6.0, and 2 mM EDTA (∼1:2 w/v) and passed three times through a French press. The insoluble fraction, which contains the membrane proteins, was harvested by centrifugation (130,000*g*, 1 h, 4 °C) and solubilized overnight at 4 °C in 4 M NaCl, 50 mM MES at pH 6.0, and 2% (w/v) DM (Anatrace) in the same volume as before. To fractionate from insoluble material, an additional centrifugation step was performed. The soluble extract was applied to a chromatography column with Ni-NTA agarose (Qiagen) equilibrated with 4 M NaCl, 50 mM MES at pH 6.0, and 0.05% (w/v) DM. Three washing steps were performed: (i) with 10 bed volumes of the buffer used for equilibration, then (ii) with the same buffer plus 20 mM imidazole, and finally (iii) with 10 bed volumes of the buffer without imidazole. Elution was done in the buffer at pH 4.5, and the eluate was immediately diluted with buffer at pH 6.0 to have the final pH in the range of 5.5−6.0. The ratio between the absorption of the protein aromatic residues at 280 nm and the absorbance of the bound chromophore at 587 nm was in the range of 1.6−1.8, which is a typical value for pure SRI samples (*23*, *24*). The A_{280}/A_{587} ratio for the fusion proteins was slightly increased and was in the range of 2.0−2.2.

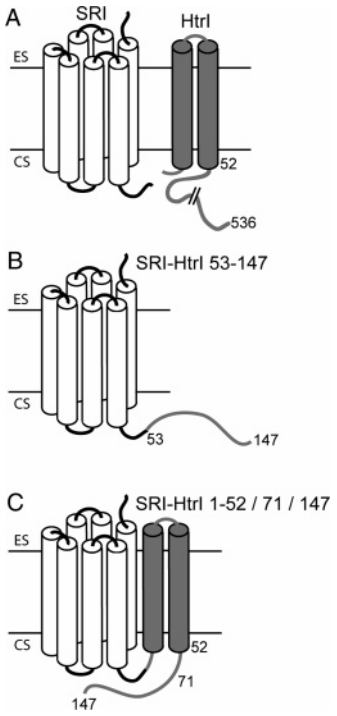

FIGURE 1: Illustration of the SRI-HtrI fusion constructs engineered and used in this study. TM1 and TM2 correspond to the TM helices of HtrI. ES and CS denote the extracellular and the cytoplasmic surfaces, respectively. The numbers correspond to the positions in the amino acid sequence of HtrI. (A) The light receptor SRI and the wild-type transducer HtrI. (B) Fusion construct where the amino acid sequence 53−147 was genetically appended to the C-terminus of SRI. (C) Fusion construct of SRI with the polypeptide of HtrI truncated at various lengths (1−52, 1−71, or 1−147).

Reconstitution of SRI and SRI-HtrI Fusions into Halobacterial Polar Lipids. To investigate the proteins under more native-like conditions, they were reconstituted into polar

lipids of purple membranes from *H. salinarum*. Reconstitution was performed as described for SRII from *H. salinarum* (*25*). The protein complex reconstituted into polar lipids was pelleted (5,200*g*, 10 min, 4 °C) and resuspended in 4 M NaCl and 100 mM Tris-maleic acid at the desired pH. The efficacy of reconstitution was evaluated by centrifugation: the exchange of detergent versus lipids was considered successful when the blue protein moved into the pellet fraction and the supernatant became colorless. Gel electrophoresis (data not shown) revealed that the proteins were exclusively in the membrane-containing pellet. More than 80% of the protein molecules retained the chromophore as judged by the ratio of A_{587} before and after reconstitution.

Time-Resolved UV/Vis Spectroscopy. Absorption spectra were recorded on a UV-2401 PC (Shimadzu) spectrophotometer in the dark. All samples were measured in a 1-cm cell with the temperature adjusted to 20 °C by a circulating water bath. An LED (Luxeon Star) with the emission maximum at 589 nm (21 nm FWHM) and an intensity of 6.7 mW/cm^2 was used for light excitation of the protein. After 2−3 s of illumination, the recovery kinetics of the ground state was monitored at 590 nm. 15 to 25 datasets were collected and averaged for each pH value.

ATR-FT-IR Difference Spectroscopy. A suspension of freshly reconstituted protein in 10 mM NaP at pH 6.0 was dried on the surface of a diamond internal reflection element under a stream of nitrogen gas. Then, the protein film was immersed in a solution of 4 M NaCl and 100 mM Tris-maleic acid at pH 5.5 or pD 5.1 for several hours. FT-IR difference spectra were acquired at 20 °C using a temperature-controlled ATR-IR cell mounted in the sample chamber of the FT-IR spectrometer (IFS 66v from Bruker Optics). The optical resolution was set to 4 cm^{-1}, and the spectral range was limited by an interference filter to 1800−950 cm^{-1}. The orange LED was used for sample illumination. 100 light−dark individual spectra (with 512 scans each) were averaged to improve the signal-to-noise ratio (see (*26*, *27*) for further spectroscopic details).

RESULTS

Ground-State Recovery Kinetics of SRI and the Fusion Constructs with HtrI. The pH dependence of the M state decay represents a tool to assay the interaction of the photoreceptor SRI with the transducer HtrI (*7*). In the absence of transducer, SRI exhibits a strong pH dependence on the M decay, while in the presence of HtrI this dependence is almost completely abolished. Since the M state decays directly to the ground state in the one-photon photocycle of SRI (*28*, *29*), the ground-state recovery matches the pH dependence. Ground-state recovery kinetics can be conveniently recorded at 590 nm to avoid the strong scattering from the protein−lipid aggregates when detecting the M decay at 370 nm.

The ground-state recovery kinetics of free SRI and of the various fusion proteins (see Figure 1) are depicted in Figure 2 for two different pH values (pH 5.5 and pH 7.5). In the absence of transducer, the ground-state recovery kinetics after photobleaching was drastically slowed down when changing the pH from acidic to neutral, which agrees well with previous studies on native membrane fragments (*5*, *7*, *8*, *13*, *14*). The strong pH dependence of the SRI ground-state recovery was completely suppressed when the receptor was fused to either of the two truncated HtrIs consisting of the TM helices and cytoplasmic region, SRI-HtrI 1−71 and SRI-HtrI 1−147, respectively. The recovery times for these constructs were fairly constant over the whole range of pH values used in our study (5.5 < pH < 7.5). These results demonstrate that the expression of the fusion constructs in *E. coli* and the subsequent reconstitution into halobacterial lipids yields functional SRI−HtrI complexes. The fusion construct SRI-HtrI 1−147 served as standard reference because the truncated HtrI (147 residues) is fully capable of accepting the signal from SRI when compared to the full-length HtrI (536 residues, unpublished data). Similar to free SRI, the recovery kinetics of SRI fused to the two TM helices of HtrI (SRI-HtrI 1−52) or to the C-terminal region of HtrI adjacent to the TM helices (SRI-HtrI 53−147) were pH-dependent.

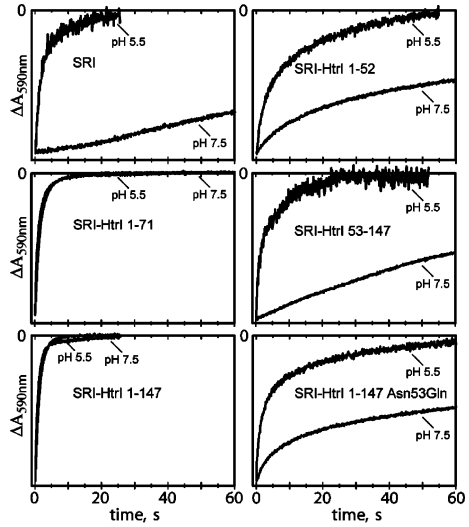

FIGURE 2: Light-induced absorbance changes monitored at 590 nm of free SRI, SRI-HtrI 1−71, SRI-HtrI 1−147, SRI-HtrI 1−52, SRI-HtrI 53−147, and SRI-HtrI 1−147 Asn53Gln reconstituted in polar lipids from halobacterial purple membranes at pH 5.5 and pH 7.5. The curves were normalized to the same initial absorbance to facilitate comparison.

Because of the importance of Asn in the interaction of the related SRII to HtrII, we focused on Asn53 as the only asparagine between positions 52 and 147 in the polypeptide chain of HtrI. Therefore, we exchanged Asn53 of HtrI to Asp, Ala, or Gln in the construct SRI-HtrI 1−147 and determined the recovery kinetics of the construct. As an example, the kinetics of the SRI-HtrI 1−147 Asn53Gln mutant is displayed in Figure 2 (bottom right panel). It is evident that the recovery kinetics at pH 5.5 (black trace) is about 10 times slower then that of SRI-HtrI 1−147. Thus, the pH-dependent kinetics of the Asn53 mutant of HtrI indicates a specific role of this residue in the interaction with the receptor. The mutants Asn53Asp and Asn53Ala exhibited essentialy the same kinetic behavior as SRI −Htr 1−147 Asn53Gln (data not shown).

FT-IR Difference Spectra of SRI and of the Fusion Constructs with HtrI. FT-IR spectra were acquired across the range of 1800 to 950 cm^{-1} under constant illumination with orange light. Experiments were carried out at pH 5.5 to ensure the same protonation state of the Schiff base counterion, Asp76 (*8*, *30*, *31*). The light-induced FT-IR difference spectra between the spectrum of the M intermedi-

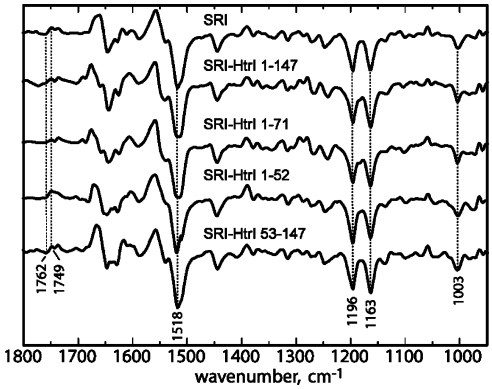

FIGURE 3: IR difference spectra (illuminated minus non-illuminated) of free SRI, SRI-HtrI 1−147, SRI-HtrI 1−71, SRI-HtrI 1−52, and SRI-HtrI 53−147 (from top to bottom) across the region of 1800 and 950 cm^{-1}. Spectra were normalized on the same intensity of the chromophoric bands at 1518 cm^{-1} and 1003 cm^{-1}. Vertical dashed lines indicate difference bands discussed in the text.

ate and that of the ground state of SRI and the fusion proteins, respectively, are presented in Figure 3. In these difference spectra, positive bands correspond to the species appearing in the M state and negative bands to the ground-state species. All spectra were very similar, confirming that M is the only intermediate trapped under photostationary conditions for all constructs used in the study. In particular, the strong chromophoric bands (*32*) appearing in the spectra of free SRI and the chimeric proteins were identical. The strongest negative band in the spectrum at 1518 cm^{-1} corresponds to the C═C stretching vibration of retinal. The two negative peaks at 1163 cm^{-1} and 1196 cm^{-1} are assigned to C−C stretching modes. The band at 1003 cm^{-1} is due to a methyl rocking vibration. Despite the identity in the chromophore modes, vibrations of the apoprotein were significantly different for the various fusion constructs. Specific changes were observed in the amide I (predominantly C═O stretch of the protein backbone, 1690−1620 cm^{-1}) and the amide II regions (coupled vibration of the C−N stretch and the N−H bend of the peptide bond, 1570−1520 cm^{-1}) as well as in the C═O carboxyl group stretch region (1800−1700 cm^{-1}) and the region associated with Asn/Gln side chain vibrations (1700−1680 cm^{-1}). The two bands at 1762(−)/1749(+) cm^{-1} have been previously assigned to the C═O stretching vibration of protonated Asp76 in SRI (*30*, *31*), which appeared in all of the difference spectra shown.

Double-difference spectra between free SRI and the fusions were calculated to visualize the influence of the transducer. The differences in the amide I and amide II regions were relatively large for the fusions SRI-HtrI 1−147 and SRI-HtrI 1−71, decreasing for the shorter fusion SRI-HtrI 1−52, and being minor for SRI-HtrI 53−147 (Figure 4, upper panel). The significance of the double differences is demonstrated by the almost flat baseline, which represents the (double) difference between two independent light-induced difference spectra of SRI-HtrI 1−147. Consequently, the vibrational features reflected in the double differences in the various fusion constructs are beyond noise. The differences in the 1300−1220 cm^{-1} region are attributed to amide III modes, which tally with those of the amide I and II changes. Other differences are related to amino acid side chain vibrations but are too premature to be assigned.

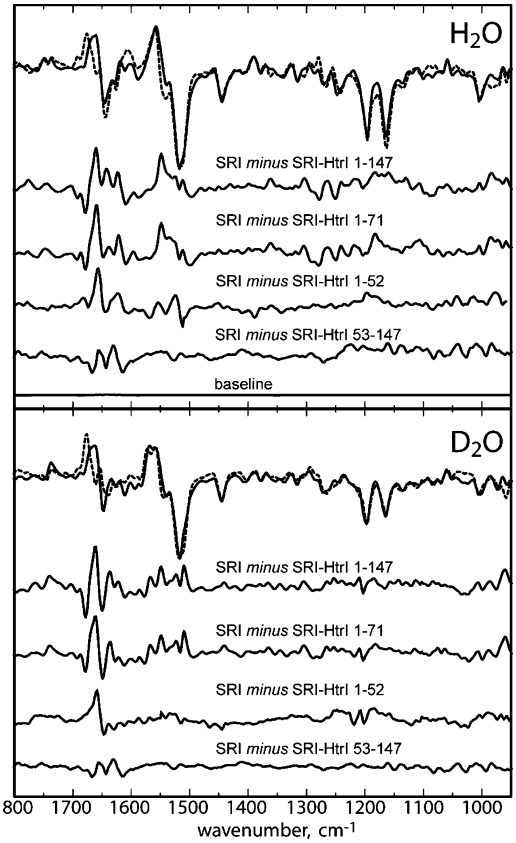

FIGURE 4: Double difference IR spectra calculated by subtraction of SRI-HtrI 1−147, SRI-HtrI 1−71, SRI-HtrI 1−52, and SRI-HtrI 53−147 from the difference spectrum of free SRI. Spectra have been recorded in H_2O (upper panel) and in D_2O (lower panel) under otherwise identical conditions. For comparison, the difference specta of free SRI (—) and SRI-HtrI 1−147 (---) are presented at the top of each panel. The bottom trace in the experiments in H_2O corresponds to a baseline where two independently recorded light-induced difference spectra of SRI-HtrI 1−147 have been subtracted. The low noise level demonstrates the significance of the detected differences in the other double difference spectra. The corresponding baseline in D_2O is comparable on this level of absorbance (not shown).

The strong background absorption from the bending mode of H_2O overlaps with the amide I band from the protein. To exclude any artifactual signals in this frequency range, difference spectra were also recorded in D_2O solution. The overall shape of the double difference spectra remained unchanged (Figure 4, lower panel), thus confirming the observations in H_2O. Remarkably, the intensities in the amide I and amide II regions, both in H_2O and D_2O, of the double difference spectrum between SRI and SRI-HtrI 1−147 can be considered as the sum of those of SRI-HtrI 1−52 and SRI-HtrI 53−147. Consequently, the conformational changes in the TM and the cytoplasmic region may occur independently from each other.

The double difference spectra in the 1800−1680 cm^{-1} region (C═O stretching vibrations of Asp, Glu, Asn, and Gln residues) are shown in Figure 5. Several differences between the two groups of mutants SRI-HtrI 1−147 and SRI-HtrI 1−71, and SRI-HtrI 1−52 and SRI-HtrI 53−147 were found in this spectral region. The two bands at 1760(−)/1747(+) cm^{-1} observed for SRI-HtrI 1−147 (black trace) and SRI-HtrI 1−71 (red trace) were not present in the spectra of SRI-HtrI 1−52 (blue trace) and SRI-HtrI 53−147 (green trace). H/D exchange downshifted these bands to 1753(−)/

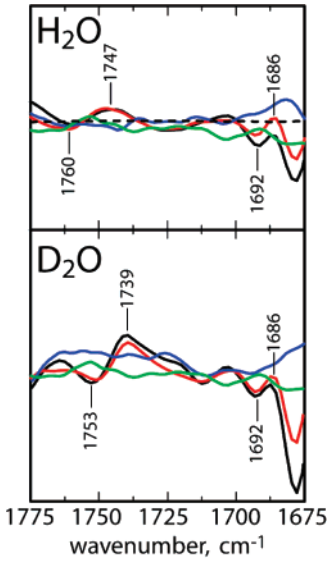

FIGURE 5: Comparison of the double difference IR spectra between SRI and SRI-HtrI 1−147 (black), SRI-HtrI 1−71 (red), SRI-HtrI 1−52 (blue) and SRI-HtrI 53−147 (green) recorded in H_2O (top) and D_2O (bottom) in the carbonyl stretching region. The dashed trace is the baseline recorded in H_2O.

1739(+) cm^{-1}, characteristic for the C═O stretching vibration from carboxylic acids. Another distinct feature in the double-difference spectra between SRI and SRI-HtrI 1−147 or SRI-HtrI 1−71 is the negative peak at 1692 cm^{-1} and the positive peak at 1686 cm^{-1} (Figure 5). These frequencies are typical of the C═O stretching mode of asparagine or glutamine side chains. The position of these bands was not sensitive to H_2O/D_2O exchange, most probably because of the inaccessibility of this particular group for H/D exchange. The analogous band of HtrII from *N. pharaonis* in the SRII−HtrII complex with the maximum at 1694 cm^{-1} has been assigned to Asn74 (*18*, *19*). A likely candidate for this role in HtrI is Asn53. If so, the absence of the 1692(−)/1686(+) cm^{-1} band in the spectrum of SRI-HtrI 1−52 is obvious; in the case of SRI-HtrI 53−147, it may be due to the lack of specific interaction between SRI and Asn53 of HtrI. To investigate the role of Asn53, point mutants have been constructed (see above) and measured by FT-IR difference spectroscopy.

IR Spectra of SRI-HtrI 1−147 with Asn53 Substitutions. Three fusion constructs were generated, where Asn53 was exchanged with Asp, Ala, or Gln. The fusion of SRI with the first 147 residues of HtrI was chosen to ensure proper folding of the membrane-proximal region upon mutation.

The M minus ground state difference spectra of the SRI-HtrI 1−147 chimeras with mutated Asn53 are displayed in Figure 6. Common to free SRI and all fusion proteins, the dominant chromophoric bands (at 1518, 1196, 1163, and 1003 cm^{-1}) are identical in frequency and intensity. However, the spectral changes in the amide I and amide II regions were closer to those observed for free SRI, indicating similar conformational transition upon light excitation.

In order to compare the spectral changes occurring in the 1800−1680 cm^{-1} region in SRI-HtrI 1−147 with Asn53 substitutions, double differences between free SRI and the corresponding fusions were analyzed. Two important features were thus visualized (Figure 7): (i) The bands at 1760(−)/1747(+) cm^{-1} of SRI-HtrI 1−147 (black trace) disappeared upon substitution of Asn53, and (ii) the bands at 1692(−)/1686(+) cm^{-1} were completely absent in the Asn53Asp (red trace) and Asn53Ala mutations (blue trace), while the Asn53Gln mutation (green trace) lowered the amplitude of the differential band feature.

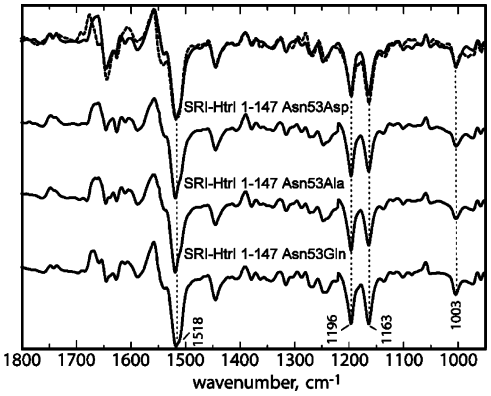

FIGURE 6: IR difference spectra of free SRI (—), SRI-HtrI 1−147 (---), SRI-HtrI 1−147 Asn53Asp, SRI-HtrI 1−147 Asn53Ala, and SRI-HtrI 1−147 Asn53Gln in the region between 1800 and 950 cm^{-1}. All spectra were scaled on the intensities of the chromophoric bands at 1518 cm^{-1} and 1003 cm^{-1}. Vertical dashed lines indicate the difference bands discussed in the text.

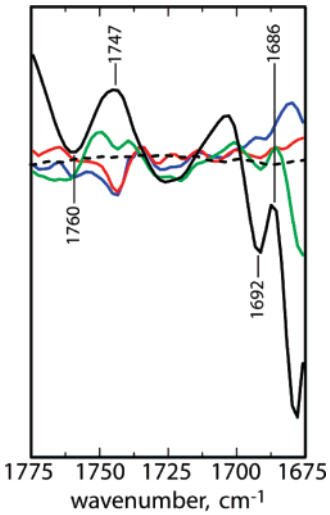

FIGURE 7: Comparison of the double difference IR spectra of SRI *minus* SRI-HtrI 1−147 (black), SRI-HtrI 1−147 Asn53Asp (red), Asn53Ala (blue), and Asn53Gln (green) in the carbonyl stretching region. Again, the dashed trace is the baseline.

DISCUSSION

The interaction between SRI and its cognate transducer HtrI was investigated by constructing fusion chimeras of SRI and HtrI of different length. The variation in the transducer's structure influences the photocycle kinetics of the complex as determined by time-resolved spectroscopy in the visible wavelength range as well as the associated structural changes as gauged by FT-IR difference spectroscopy. The design of the chimeras was based on earlier studies, which located the interaction sites between receptor and transducer in the membrane (*14*) and membrane-proximal (*8*) regions. Two sets of HtrI deletion mutants were chosen according to their ability to close or not close the proton channel of SRI (*8*), which allowed us to investigate the properties of the receptor−transducer complex and characterize the first step of signal transduction.

SRI-HtrI Fusion Chimeras Are Functional after Liposome Reconstitution. Heterologous high-yield expression systems such as *E. coli*, offer an effective, fast and easy way to produce large amounts of SRI (*23*). However, the protein must be solubilized in detergent and subsequently reconstituted in halobacterial lipids mimicing the native environment. The reconstitution procedure used in this work has been successfully employed in the characterization of SRII from *H. salinarum* (*25*) as well as in crystallization (*10, 11*), EPR (*33*), and FT-IR (*16, 19*) studies of the SRII−HtrII complex from *N. pharaonis*.

The ground-state recovery kinetics of free SRI reconstituted into polar lipids of purple membranes followed exponential pH dependence for the M state but with somewhat slower characteristic times than those of the native *H. salinarum* membranes (*7, 8*). The slight change in the photocycle kinetics is most probably due to the different lipid compositions used, as was previously reported for bacteriorhodopsin (*34*) and for SRI reconstituted into phosphatidylglycerol liposomes (*24*). The fusion of the HtrI fragments 1−147 or 1−71 led to the recovery rates corresponding to those established for analogous constructs under native conditions (*8*). Thus, functional interaction with transducer minimizes the influence of the environment on the receptor. On the basis of the pH dependencies of the ground-state recovery kinetics of the reconstituted SRI and the SRI-HtrI fusion proteins, we conclude that the reconstitution procedure does not hamper their functionality.

pH (In)Dependence of the Ground-State Recovery Kinetics Correlates with Light-Induced Conformational Changes in the SRI−HtrI Complex. Despite the identity in the chromophore modes, the vibrations of the apoprotein were significantly different for the fusions of different length (Figure 3). The double-difference FT-IR spectra (Figure 4) between free SRI and the fusion proteins upon light excitation showed prominent bands in the amide I region for SRI-HtrI 1−147 and SRI-HtrI 1−71, whereas those for the shorter fusion, SRI-HtrI 1−52, were substantially weaker. This contrasts with the homologous SRII−HtrII system, where the shorter fusion protein (SRII-HtrII 1−120) has been reported to show higher intensities in the amide I region (*19*) than the longer one (SRII-HtrII 1−147) (*16*). Interestingly, the presence of the cytoplasmic extension alone, that is, in the absence of the TM domain, resulted in relatively small conformational changes as derived from the double-difference spectrum of SRI and the fusion construct SRI-HtrI 53−147 (Figure 4), which showed only minor amide I absorption differences. This fact is in excellent agreement with our results from the kinetics of the ground-state recovery and previous findings that the membrane-proximal region of HtrI devoid of the TM domain is incapable of closing the proton channel of SRI (*8*).

Thus, the extent of the conformational changes in the SRI−HtrI complex depends on the presence of the membrane-proximal as well as the TM domain of HtrI. The fusions of SRI and HtrI fragments incapable of closing the receptor's proton channel underwent almost the same conformational changes as free SRI. However, when SRI was fused to the transducer deletion mutants exhibiting pH-independent ground-state recovery kinetics, SRI-HtrI 1−147 and SRI-HtrI 1−71, relatively large conformational changes were detected in the complex (Figure 4). On the basis of the above facts, we conclude that the observed confomational changes are indeed associated with the signal transfer from SRI to HtrI.

Origin of the 1760(−)/1747(+) cm^{-1} Bands in the Functional SRI−HtrI Complexes. Upon light excitation, two bands at 1760(−)/1747(+) cm^{-1} appear in the double difference FT-IR spectra between free SRI and the fusion proteins SRI-HtrI 1−147 and SRI-HtrI 1−71, respectively (upper panel of Figure 5, black and red traces, respectively). The characteristic downshift of the bands to 1753(−)/1739(+) cm^{-1} in D_2O demonstrates that this group is accessible to the bulk solvent (lower panel of Figure 5). Examination of the same spectral region under identical conditions revealed no significant changes for SRI-HtrI 1−52 and SRI-HtrI 53−147 (Figure 5, blue and green traces, respectively). Since SRI-HtrI 1−147 and SRI-HtrI 1−71 are functional in terms of the suppression of the pH dependence of the ground-state recovery, the occurrence of the bands at 1760(−)/1747(+) cm^{-1} is most probably due to the changes in the environment of Asp76 resulting in the shift of its pK_a. The bands of the double-difference spectra between free SRI and SRI-HtrI 1−147 and SRI-HtrI 1−71 appear at 1760(−)/1747(+) cm^{-1}, respectively, that is, virtually at the same wavenumbers where the bands of Asp76 have been observed in the difference spectra. It is, thus, logical to assume that Asp76 is protonated at pH 5.5 not only in free SRI (*30*) but also in the transducer-bound form, where the pK_a of this residue is increased (*8*).

Asn53 of HtrI Is Functionally Relevant for the SRI−HtrI Complex. The bands at 1692(−)/1686(+) cm^{-1} in the double difference spectra of SRI-HtrI 1−71 and SRI-HtrI 1−147 were yet unassigned. In the homologous SRII−HtrII system from *N. pharaonis*, a similar band has been observed at 1694 cm^{-1}, which has been assigned to the C═O stretching vibration of Asn74 of HtrII (*18, 19*). Asn74 forms a stable hydrogen bond with Tyr199 of SRII (*10*), which is not disrupted even in the M state of the complex (*11*). Thus, the homologous Asn53 of HtrI was chosen for site-directed mutagenesis as a potential hydrogen-bonding residue. According to the sequence alignment (*22*), this residue is predicted to be on the cytoplasmic end of the second TM helix of HtrI, while Asn74 of HtrII from *N. pharaonis* is in the middle of the second helix.

Upon mutation, the band feature at 1692(−)/1686(+) cm^{-1} completely disappeared in the double difference spectra between SRI and SRI-HtrI 1−147 Asn53Asp and Asn53Ala, but was still detectable in SRI-HtrI 1−147 Asn53Gln, though with much lower amplitudes (Figure 7). On the basis of these results, it is tempting to assign the differential band feature at 1692(−)/1686(+) cm^{-1} to the frequency shift of the C═O stretch of Asn53 provoked by a change in interaction of the latter residue with an amino acid side chain of SRI. However, the loss of function as derived from the pH dependence of the ground-state recovery kinetics upon Asn53 mutations made the band assignment impossible. The presence of the same band of lower intensity in the spectra of the Asn53Gln mutant may only indirectly confirm that its appearance is related to changes in hydrogen bonding of Asn53 upon light excitation.

The introduction of these point mutations was also coupled to the disappearance of the bands at 1760(−)/1747(+) cm^{-1} in all of the double difference spectra. This experimental fact provides evidence for the influence of Asn53 of HtrI

with Asp76 of SRI. Remarkably, the kinetics of the ground-state recovery of all Asn53 mutants followed the pattern characteristic for free SRI, indicating Schiff base reprotonation by external protons even when both TM helices and the cytoplasmic part of the transducer are present, which is usually sufficient to abolish the pH dependence of the ground-state recovery in the wild-type complex.

In summary, our experimental data suggest that Asn53 is a crucial residue in the interaction of HtrI with SRI and their mutual interaction in the SRI−HtrI complex. This gives reasons why HtrI with the Asn53Ile phenotype has been reported to provide very little or no phototactic response when expressed in wild-type *H. salinarum* (*35*).

ACKNOWLEDGMENT

We thank Ilona Ritter, Ramona Justinger, and Christian Baeken (Jülich) for excellent technical assistance and Dr. Ionela Radu (Bielefeld) for critical discussions.

REFERENCES

1. Blanck, A., Oesterhelt, D., Ferrando, E., Schegk, E. S., and Lottspeich, F. (1989) Primary structure of sensory rhodopsin I, a prokaryotic photoreceptor, *EMBO J. 8*, 3963−3971.
2. Schäfer, G., Engelhard, M., and Müller, V. (1999) Bioenergetics of the archaea, *Microbiol. Mol. Biol. Rev. 63*, 570−620.
3. Hoff, W. D., Jung, K. H., and Spudich, J. L. (1997) Molecular mechanism of photosignaling by archaeal sensory rhodopsins, *Annu. Rev. Biophys. Biomol. Struct. 26*, 223−258.
4. Yao, V. J., and Spudich, J. L. (1992) Primary structure of an archaebacterial transducer, a methyl-accepting protein associated with sensory rhodopsin I, *Proc. Natl. Acad. Sci. U.S.A. 89*, 11915−11919.
5. Chen, X., and Spudich, J. L. (2002) Demonstration of 2:2 stoichiometry in the functional SRI-HtrI signaling complex in Halobacterium membranes by gene fusion analysis, *Biochemistry 41*, 3891−3896.
6. Krah, M., Marwan, W., Vermeglio, A., and Oesterhelt, D. (1994) Phototaxis of *Halobacterium salinarium* requires a signalling complex of sensory rhodopsin I and its methyl-accepting transducer HtrI, *EMBO J. 13*, 2150−2155.
7. Spudich, E. N., and Spudich, J. L. (1993) The photochemical reactions of sensory rhodopsin I are altered by its transducer, *J. Biol. Chem. 268*, 16095−16097.
8. Chen, X., and Spudich, J. L. (2004) Five residues in the HtrI transducer membrane-proximal domain close the cytoplasmic proton-conducting channel of sensory rhodopsin I, *J. Biol. Chem. 279*, 42964−42969.
9. Sasaki, J., and Spudich, J. L. (2000) Proton transport by sensory rhodopsins and its modulation by transducer-binding, *Biochim. Biophys. Acta 1460*, 230−239.
10. Gordeliy, V. I., Labahn, J., Moukhametzianov, R., Efremov, R., Granzin, J., Schlesinger, R., Büldt, G., Savopol, T., Scheidig, A. J., Klare, J. P., and Engelhard, M. (2002) Molecular basis of transmembrane signalling by sensory rhodopsin II-transducer complex, *Nature 419*, 484−487.
11. Moukhametzianov, R., Klare, J. P., Efremov, R., Baeken, C., Goppner, A., Labahn, J., Engelhard, M., Buldt, G., and Gordeliy, V. I. (2006) Development of the signal in sensory rhodopsin and its transfer to the cognate transducer, *Nature 440*, 115−119.
12. Krah, M., Marwan, W., and Oesterhelt, D. (1994) A cytoplasmic domain is required for the functional interaction of SRI and HtrI in archaeal signal transduction, *FEBS Lett. 353*, 301−304.
13. Perazzona, B., Spudich, E. N., and Spudich, J. L. (1996) Deletion mapping of the sites on the HtrI transducer for sensory rhodopsin I interaction, *J. Bacteriol. 178*, 6475−6478.
14. Zhang, X. N., Zhu, J. Y., and Spudich, J. L. (1999) The specificity of interaction of archaeal transducers with their cognate sensory rhodopsins is determined by their transmembrane helices, *Proc. Natl. Acad. Sci. U.S.A. 96*, 857−862.
15. Sudo, Y., Okuda, H., Yamabi, M., Fukuzaki, Y., Mishima, M., Kamo, N., and Kojima, C. (2005) Linker region of a halobacterial transducer protein interacts directly with its sensor retinal protein, *Biochemistry 44*, 6144−6152.
16. Bergo, V., Spudich, E. N., Spudich, J. L., and Rothschild, K. J. (2003) Conformational changes detected in a sensory rhodopsin II-transducer complex, *J. Biol. Chem. 278*, 36556−36562.
17. Furutani, Y., Sudo, Y., Kamo, N., and Kandori, H. (2003) FTIR spectroscopy of the complex between pharaonis phoborhodopsin and its transducer protein, *Biochemistry 42*, 4837−4842.
18. Furutani, Y., Kamada, K., Sudo, Y., Shimono, K., Kamo, N., and Kandori, H. (2005) Structural changes of the complex between pharaonis phoborhodopsin and its cognate transducer upon formation of the m photointermediate, *Biochemistry 44*, 2909−2915.
19. Bergo, V. B., Spudich, E. N., Rothschild, K. J., and Spudich, J. L. (2005) Photoactivation perturbs the membrane-embedded contacts between sensory rhodopsin II and its transducer, *J. Biol. Chem. 280*, 28365−28369.
20. Ferrando-May, E., Brustmann, B., and Oesterhelt, D. (1993) A C-terminal truncation results in high-level expression of the functional photoreceptor sensory rhodopsin I in the archaeon *Halobacterium salinarium*, *Mol. Microbiol. 9*, 943−953.
21. Barik, S. (1997) Mutagenesis and gene fusion by megaprimer PCR, *Methods Mol. Biol. 67*, 173−182.
22. Le, Moual, H., and Koshland, D. E., Jr. (1996) Molecular evolution of the C-terminal cytoplasmic domain of a superfamily of bacterial receptors involved in taxis, *J. Mol. Biol. 261*, 568−585.
23. Schmies, G., Chizhov, I., and Engelhard, M. (2000) Functional expression of His-tagged sensory rhodopsin I in *Escherichia coli*, *FEBS Lett. 466*, 67−69.
24. Krebs, M. P., Spudich, E. N., and Spudich, J. L. (1995) Rapid high-yield purification and liposome reconstitution of polyhistidine-tagged sensory rhodopsin I, *Protein Expression Purif. 6*, 780−788.
25. Mironova, O. S., Efremov, R. G., Person, B., Heberle, J., Budyak, I. L., Buldt, G., and Schlesinger, R. (2005) Functional characterization of sensory rhodopsin II from *Halobacterium salinarum* expressed in Escherichia coli, *FEBS Lett. 579*, 3147−3151.
26. Friedrich, T., Geibel, S., Kalmbach, R., Chizhov, I., Ataka, K., Heberle, J., Engelhard, M., and Bamberg, E. (2002) Proteorhodopsin is a light-driven proton pump with variable vectoriality, *J. Mol. Biol. 321*, 821−838.
27. Nyquist, R. M., Heitbrink, D., Bolwien, C., Wells, T. A., Gennis, R. B., and Heberle, J. (2001) Perfusion-induced redox differences in cytochrome c oxidase: ATR/FT-IR spectroscopy, *FEBS Lett. 505*, 63−67.
28. Swartz, T. E., Szundi, I., Spudich, J. L., and Bogomolni, R. A. (2000) New photointermediates in the two photon signaling pathway of sensory rhodopsin-I, *Biochemistry 39*, 15101−15109.
29. Szundi, I., Swartz, T. E., and Bogomolni, R. A. (2001) Multicolored protein conformation states in the photocycle of transducer-free sensory rhodopsin-I, *Biophys. J. 80*, 469−479.
30. Rath, P., Olson, K. D., Spudich, J. L., and Rothschild, K. J. (1994) The Schiff base counterion of bacteriorhodopsin is protonated in sensory rhodopsin I: spectroscopic and functional characterization of the mutated proteins D76N and D76A, *Biochemistry 33*, 5600−5606.
31. Rath, P., Spudich, E., Neal, D. D., Spudich, J. L., and Rothschild, K. J. (1996) Asp76 is the Schiff base counterion and proton acceptor in the proton- translocating form of sensory rhodopsin I, *Biochemistry 35*, 6690−6696.
32. Bousche, O., Spudich, E. N., Spudich, J. L., and Rothschild, K. J. (1991) Conformational changes in sensory rhodopsin I: similarities and differences with bacteriorhodopsin, halorhodopsin, and rhodopsin, *Biochemistry 30*, 5395−5400.
33. Bordignon, E., Klare, J. P., Doebber, M., Wegener, A. A., Martell, S., Engelhard, M., and Steinhoff, H. J. (2005) Structural analysis of a HAMP domain: the linker region of the phototransducer in complex with sensory rhodopsin II, *J Biol. Chem 280*, 38767−38775.
34. Dracheva, S., Bose, S., and Hendler, R. W. (1996) Chemical and functional studies on the importance of purple membrane lipids in bacteriorhodopsin photocycle behavior, *FEBS Lett. 382*, 209−212.
35. Jung, K. H., and Spudich, J. L. (1998) Suppressor mutation analysis of the sensory rhodopsin I-transducer complex: insights into the color-sensing mechanism, *J. Bacteriol. 180*, 2033−2042.

BI700563F